Infrared and Raman spectroscopic characterization of the borate mineral colemanite – CaB$_3$O$_4$(OH)$_3$·H$_2$O – implications for the molecular structure

Ray L. Frost [a,*], Yunfei Xi [a], Ricardo Scholz [b], Fernanda Maria Belotti [c], Mauro Cândido Filho [d]

[a] School of Chemistry, Physics and Mechanical Engineering, Science and Engineering Faculty, Queensland University of Technology, GPO Box 2434, Brisbane Queensland 4001, Australia
[b] Geology Department, School of Mines, Federal University of Ouro Preto, Campus Morro do Cruzeiro, Ouro Preto, MG 35400-00, Brazil
[c] Federal University of Itajubá, Campus Itabira, Itabira, MG 35903-087, Brazil
[d] Mining Engineer Department, School of Mines, Federal University of Ouro Preto, Campus Morro do Cruzeiro, Ouro Preto, MG 35400-00, Brazil

HIGHLIGHTS

▶ We have studied the molecular structure of colemanite.
▶ Colemanite is a secondary borate mineral formed from borax.
▶ Colemanite contains endless chains of interlocking BO$_2$(OH) triangles and BO$_3$(OH) tetrahedrons.
▶ It is important to characterize borate minerals because of the very wide range of applications.

ARTICLE INFO

ABSTRACT

Colemanite CaB$_3$O$_4$(OH)$_3$·H$_2$O is a secondary borate mineral formed from borax and ulexite in evaporate deposits of alkaline lacustrine sediments. The basic structure of colemanite contains endless chains of interlocking BO$_2$(OH) triangles and BO$_3$(OH) tetrahedrons with the calcium, water and extra hydroxide units interspersed between these chains. The Raman spectra of colemanite is characterized by an intense band at 3605 cm^{-1} assigned to the stretching vibration of OH units and a series of bands at 3182, 3300, 3389 and 3534 cm^{-1} assigned to water stretching vibrations. Infrared bands are observed in similar positions. The BO stretching vibrations of the trigonal and tetrahedral boron are characterized by Raman bands at 876, 1065 and 1084 cm^{-1}. The OBO bending mode is defined by the Raman band at 611 cm^{-1}. It is important to characterize the very wide range of borate minerals including colemanite because of the very wide range of applications of boron containing minerals.

© 2012 Elsevier B.V. All rights reserved.

1. Introduction

Approximately 60% of world boron ores are located in Turkey, mainly in Anatolia. Boron is founds in borates of metals, especially of calcium and sodium [1]. Colemanite is a common and complex inoborate mineral with general chemical formula given as CaB$_3$O$_4$(OH)$_3$·H$_2$O [2]. It crystallizes in the monoclinic system, $P2_1/a$ space group, with unit cell parameters a = 8.7712 Å, b = 11.247 Å, c = 6.091 Å and β = 110.12° [3]. Its crystal structure contains infinite boron–oxygen chains parallel to the a axis. The chain elements consist of two BO$_4$ tetrahedra and a ring of the composition [B$_3$O$_4$(OH)$_3$]$^{2-}$. The chains are joined to each other laterally by ionic bonds through the Ca^{2+} ions to form sheets extending parallel to (010). A system of hydrogen bonds involving the hydroxyl groups in the chain and the water molecules ties the sheets together [4]. Colemanite is usually applied in the production of boric acid, but it is still used in the production of borax, borax hydrates and sodium perborates. Nowadays, the productions of boron compounds have increased because of their demand in nuclear technology, in the glass and ceramic industry, as abrasive and refractors, in agriculture, among others [1,5,6]. In recent study colemanite ore waste was applied in the Portland cement production [7]. In the environmental sciences, the mineral was applied in the water treatment [8].

In the borate-producing countries, the borate ore deposits were formed by a supergene type of deposition and comprise low to moderately water-soluble borate salts. Boric acid and borate salts enrichments of supergene type occur within these environments: (a) volcanic emanations and hot springs; (b) marine evaporates; (c) recent playas, pan and saline flats in hot arid climates; (d) recent saline–alkaline lakes in cold arid climates; and (e) tertiary

* Corresponding author. Tel.: +61 7 3138 2407; fax: +61 7 3138 1804.
E-mail address: r.frost@qut.edu.au (R.L. Frost).

through Pleistocene saline–alkaline lake deposits. The three most important borate deposits belong to the latter type of deposit, where we found volcanically derived material contributing to the composition of the borates and their host rock [9].

The name colemanite was given by the discoverer of the mineral in honor of William T. Coleman, who has been identified with the borax interests of the Pacific Coast from the commencement [10]. Despites the type locality in Furnace Creek District, colemanite was described from a number of localities, including Kirka and Bigadiç deposits in Turkey, Loma Blanca and Esperanza deposits in Argentina [11] and Millstream deposits in Canada [12].

Vibrational spectroscopy has been applied to borate glasses [13–16]. There have been a number of studies of borate glasses doped with a wide range of radioactive atoms [17,18]. Borate glasses are used as a means of containment of radioactive materials. There have been a number of studies looking at the effect of radiation on borate glasses [19,20]. If there is to be an understanding of borate glasses and their role in radioactive element containment, then an understanding of the vibrational spectroscopy of borate minerals needs to be undertaken. The number of vibrational spectroscopic studies of borate minerals is quite few and far between [21–24]. The number of Raman studies of borate minerals is also very limited [25,26]. There have been a number of infrared studies of some natural borates [27–30]. Most of these references are not new and there have been no recent studies on the vibrational spectroscopy of natural borates. Ross in Farmer's treatise reported the infrared spectra of several borate minerals [31]. The use of infrared spectroscopy is limited by the spatial resolution of the technique which is around 25 μm. In comparison, the spatial resolution using Raman spectroscopy is 1 μm. Thus, when studying a mineral using spectroscopic techniques it is advantageous to use Raman spectroscopy. The selection of the target mineral is more easily made. With infrared spectroscopy, any impurities will be measured as well as the target mineral.

Raman spectroscopy has proven most useful for the study of secondary minerals [26,32–37]. To the best of the authors' knowledge, there have been very few vibrational spectroscopic studies of borate minerals [38–42]. A Raman and infrared spectrum of colemanite may be found on the RRUFF data base at http://rruff.info/colemanite/display=default/R050102, however, no interpretation is given.

Raman studies of this natural mineral have been forthcoming. The objective of this paper is to report the vibrational spectroscopic study of a natural colemanite mineral and relate the spectra to the molecular chemistry and the crystal chemistry of this borate mineral. We have characterized colemanite using Raman and infrared spectroscopy.

2. Experimental

2.1. Samples description and preparation

The colemanite sample studied in this work was obtained from the collection of the Geology Department of the Federal University of Ouro Preto, Minas Gerais, Brazil, with sample code SAA-130. The sample is from the type locality for the mineral, the Inyo Co., located in the Death Valley, California USA.

The borate mineral deposit in the Death Valley are related to the Miocene–Pliocene Furnace Creek Formation, deposited in marginal lacustrine and lacustrine environments in an extensional setting. The bedded borate facies comprises bodies of borate, mainly colemanite. Other minerals are ulexite, probertite, gypsum and anhydrite (Tanner 2002).

The sample was gently crushed and the associated minerals were removed under a stereomicroscope Leica MZ4. The colemanite sample was phase analyzed by X-ray diffraction. Scanning electron microscopy (SEM) was applied to support the mineralogical chemical.

2.2. Scanning electron microscopy (SEM)

Experiments and analyses involving electron microscopy were performed in the Center of Microscopy of the Universidade Federal de Minas Gerais, Belo Horizonte, Minas Gerais, Brazil (http://www.microscopia.ufmg.br).

Colemanite single crystal was coated with a 5 nm layer of evaporated Au. Secondary Electron and Backscattering Electron images were obtained using a JEOL JSM-6360LV equipment. Qualitative and semi-quantitative chemical analysis in the EDS mode were performed with a ThermoNORAN spectrometer model Quest and was applied to support the mineral characterization.

2.3. Raman microprobe spectroscopy

Crystals of colemanite were placed on a polished metal surface on the stage of an Olympus BHSM microscope, which is equipped with 10×, 20×, and 50× objectives. The microscope is part of a Renishaw 1000 Raman microscope system, which also includes a monochromator, a filter system and a CCD detector (1024 pixels). The Raman spectra were excited by a Spectra-Physics model 127 He–Ne laser producing highly polarized light at 633 nm and collected at a nominal resolution of 2 cm^{-1} and a precision of ±1 cm^{-1} in the range between 200 and 4000 cm^{-1}. Repeated acquisitions on the crystals using the highest magnification (50×) were accumulated to improve the signal to noise ratio of the spectra. Raman Spectra were calibrated using the 520.5 cm^{-1} line of a silicon wafer. The Raman spectrum of at least 10 crystals was collected to ensure the consistency of the spectra.

2.4. Infrared spectroscopy

Infrared spectra were obtained using a Nicolet Nexus 870 FTIR spectrometer with a smart endurance single bounce diamond ATR cell. Spectra over the 4000–525 cm^{-1} range were obtained by the co-addition of 128 scans with a resolution of 4 cm^{-1} and a mirror velocity of 0.6329 cm/s. Spectra were co-added to improve the signal to noise ratio.

Spectral manipulation such as baseline correction/adjustment and smoothing were performed using the Spectracalc software package GRAMS (Galactic Industries Corporation, NH, USA). Band component analysis was undertaken using the Jandel 'Peakfit' software package that enabled the type of fitting function to be selected and allows specific parameters to be fixed or varied accordingly. Band fitting was done using a Lorentzian–Gaussian cross-product function with the minimum number of component bands used for the fitting process. The Gaussian–Lorentzian ratio was maintained at values greater than 0.7 and fitting was undertaken until reproducible results were obtained with squared correlations of r^2 greater than 0.995.

3. Results and discussion

3.1. Chemical characterization

The SEM image of colemanite sample studied in this work is shown in Fig. 1. Colemanite crystal shows a prismatic form. Qualitative chemical composition shows a homogeneous phase, composed by Ca with minor amounts of Si. Due to the low energy emission, boron was not detected.
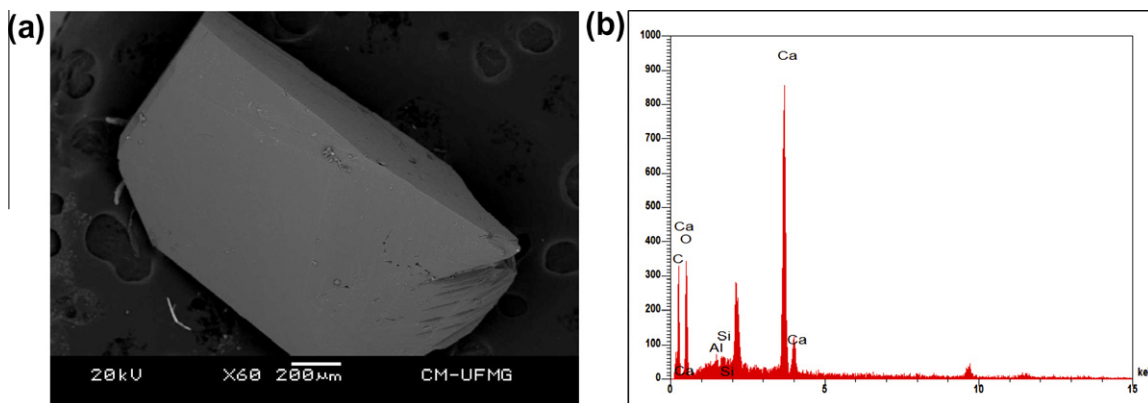
Fig. 1. (a) Backscattered electron image (BSI) of a colemanite single crystal up to 2.0 mm in length. (b) EDS spectra of colemanite.

3.2. Spectroscopy

The Raman spectrum of colemanite over the 100–4000 cm^{-1} spectral range is displayed in Fig. 2a. Significant intensity is observed in the OH stretching region and there are large parts of the spectrum where no intensity is observed. The spectrum is therefore subdivided into sections depending upon the type of vibration being studied. The infrared spectrum over the 500–4000 cm^{-1} spectral range is illustrated in Fig. 2b. Strong intensity is observed in the OH stretching region and in the BO stretching region. Since there are large parts of the spectrum where no intensity is observed, the infrared spectrum is subdivided into sections as a function of the type of vibration.

The Raman spectrum over the 800–1400 cm^{-1} spectral range is given in Fig. 3a. As Ross rightly points out the spectra of borate minerals depends heavily on the possible anions in the mineral [31]. The coordination polyhedron around the boron atom will be either a triangle or a tetrahedron. In the case of colemanite, the structure consists of linked triangles and tetrahedra. Thus for colemanite, the vibrational spectra of both structural units will be ob-

served. The spectra of colemanite are complex especially in the infrared spectrum. This is caused by the observation of bands due to four different coordination polyhedra namely BO_3^{3-}, $B(OH)_3$, BO_4^{5-}, and $B(OH)_4^-$. The Raman spectrum of colemanite shows a very intense Raman band at 1084 cm^{-1} with a shoulder at 1065 cm^{-1}. This band is assigned to the trigonal symmetric stretching mode. The two bands at 876 and 892 cm^{-1} are attributed to the symmetric stretching mode of the tetrahedral boron. A series of bands are found between 1200 and 1500 cm^{-1}. According to Ross [31] (page 220 of this reference), bands between 1300 and 1500 cm^{-1} are due to the antisymmetric stretching modes of trigonal boron. Raman bands are observed at 1154, 1257, 1301 and 1323 cm^{-1}. This concept is perhaps confirmed by the intensity of the infrared bands in the 1300–1500 cm^{-1} region (Fig. 6b).

The infrared spectrum of colemanite in the 500–1200 cm^{-1} spectral range is provided in Fig. 3b. The infrared spectrum shows much greater complexity than the equivalent Raman spectrum. The infrared bands at 1019 and 1044 cm^{-1} are the equivalent of the Raman bands at 1065 and 1084 cm^{-1}, attributed to assigned to the trigonal symmetric stretching mode. The intense infrared
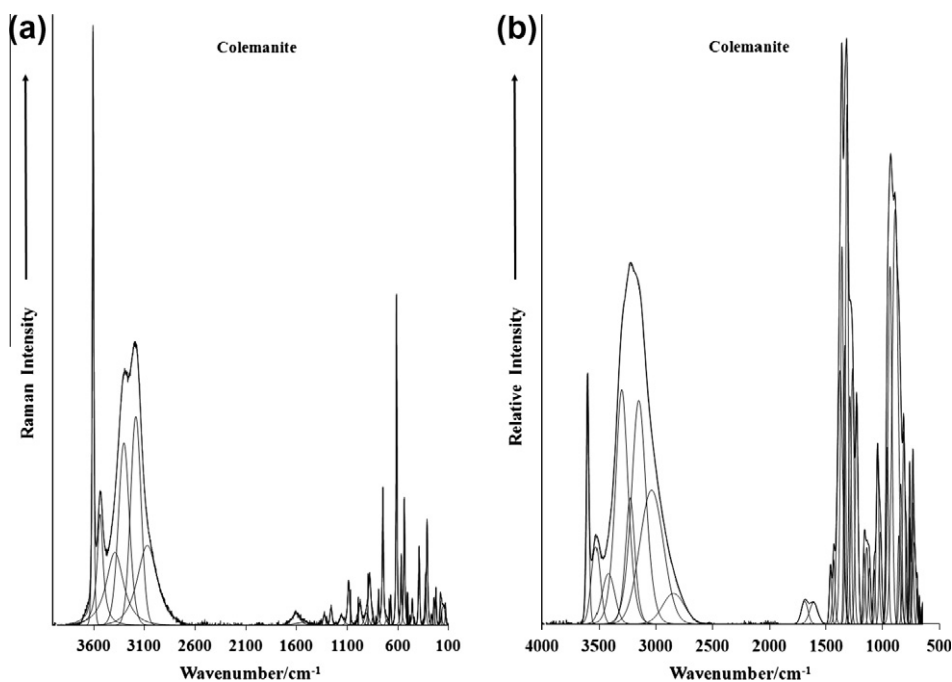

Fig. 2. (a) Raman spectrum of colemanite over the 100–4000 cm^{-1} spectral range. (b) Infrared spectrum of colemanite over the 500–4000 cm^{-1} spectral range.
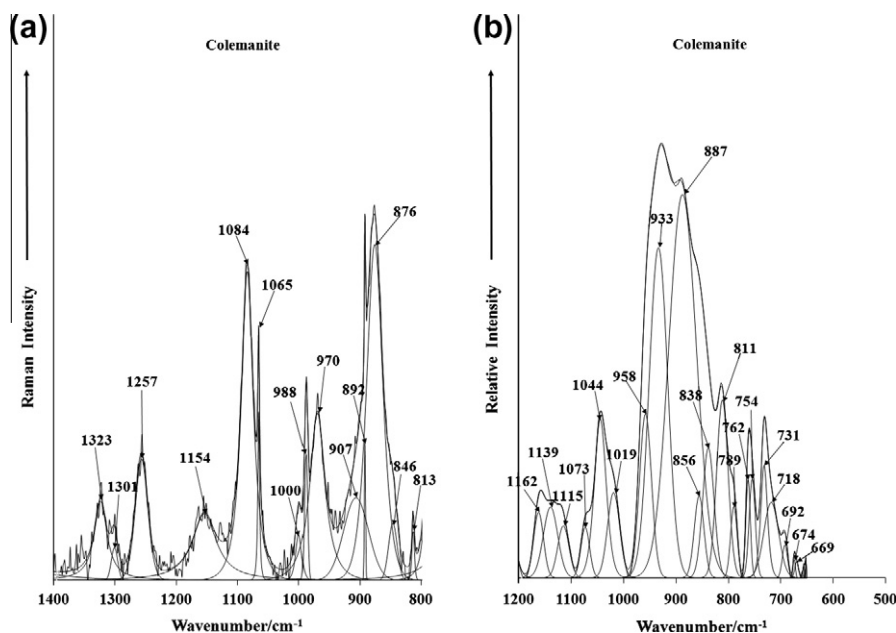
Fig. 3. (a) Raman spectrum of colemanite over the 800–1400 cm^{-1} spectral range. (b) Infrared spectrum of colemanite over the 500–1300 cm^{-1} spectral range.

bands at 887 and 933 cm^{-1} with shoulder bands at 838, 856 and 958 cm^{-1} are considered to be water librational (restricted rocking motions) bands. Equivalent Raman bands were observed at 970 and 988 cm^{-1}. The infrared spectrum of colemanite shows complexity in the 650–800 cm^{-1} with many infrared bands being observed. Infrared bands are found at 669, 674, 692, 718 and 731 cm^{-1}. These bands may be assigned to the out-of-plane BOH bending modes.

The Raman spectra in the 300–800 cm^{-1} spectral range and in the 100–300 cm^{-1} spectral region are displayed in Fig. 4a and b. The first figure is dominated by a very intense Raman band at 611 cm^{-1}. This band is attributed to the bending mode of trigonal

and tetrahedral boron. Other Raman bands of low intensity are observed at 654, 565, 669 and 684 cm^{-1} which may also be attributed to this vibrational mode. The Raman bands at 745 and 788 cm^{-1} may be assigned to the out-of-plane BOH bending modes. The Raman bands at 309, 325 and 388 cm^{-1} are attributed to CaO stretching and bending vibrations. Raman bands are observed in the 100–300 cm^{-1} spectral range and are simply described as external vibrational modes.

The Raman spectrum in the 2600–4000 cm^{-1} spectral range is reported in Fig. 5a.

A very sharp intense Raman band is observed at 3605 cm^{-1} and is assigned to the OH stretching vibration. Raman bands are ob-
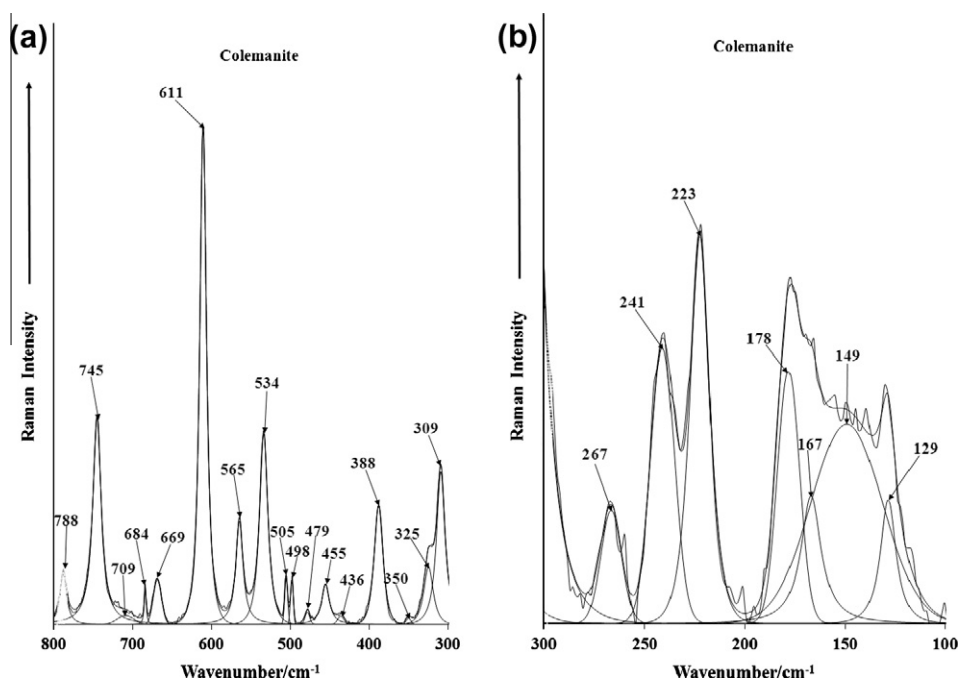

Fig. 4. (a) Raman spectrum of colemanite over the 300–800 cm^{-1} spectral range. (b) Raman spectrum of colemanite over the 100–300 cm^{-1} spectral range.
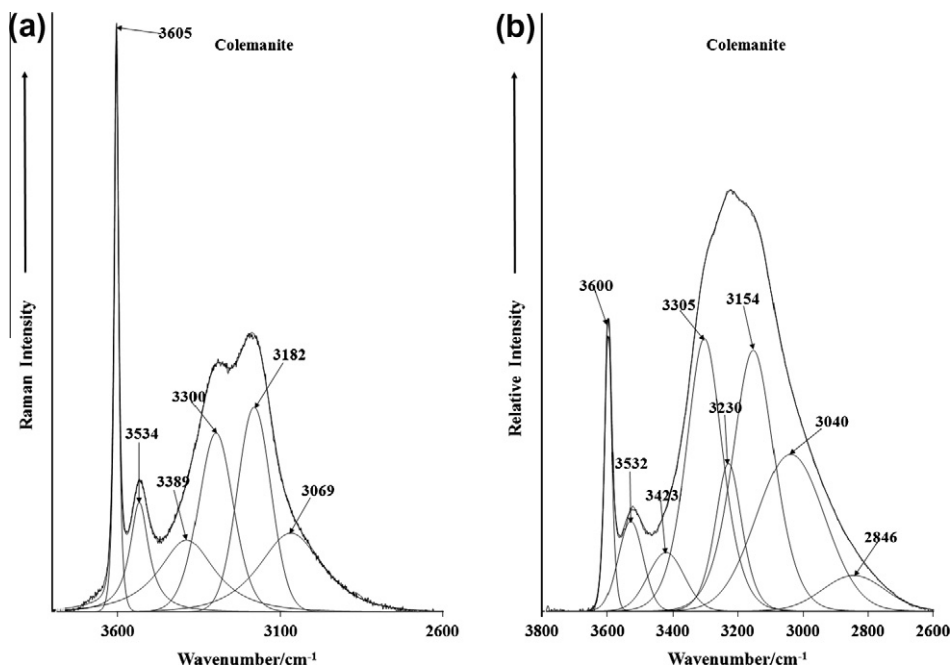
Fig. 5. (a) Raman spectrum of colemanite over the 2600–4000 cm^{-1} spectral range. (b) Infrared spectrum of colemanite over the 2600–4000 cm^{-1} spectral range.
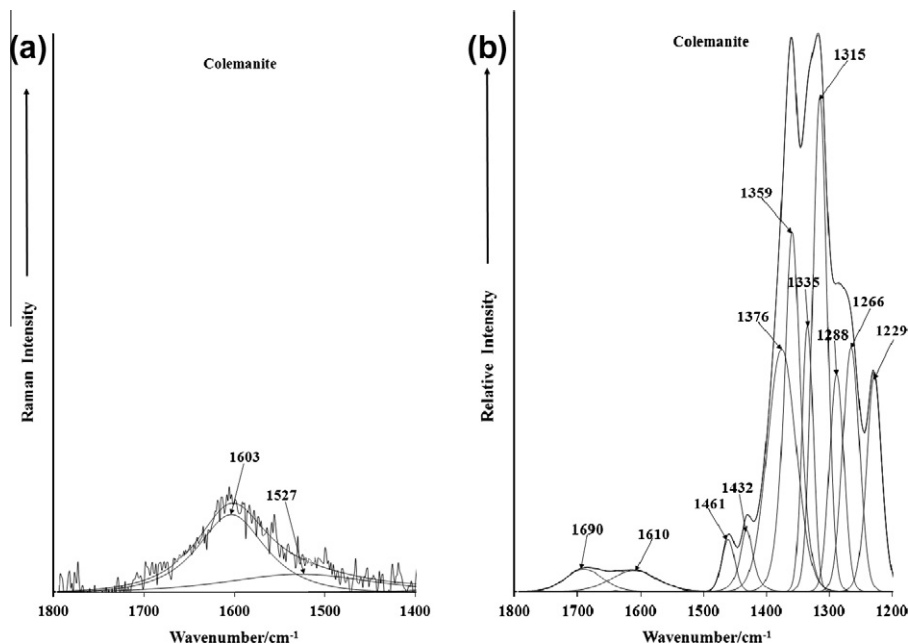

Fig. 6. (a) Raman spectrum of colemanite over the 1300–1800 cm^{-1} spectral range. (b) Infrared spectrum of colemanite over the 1300–1800 cm^{-1} spectral range.

served at 3069, 3182, 3300, 3389 and 3534 cm^{-1}. These bands are attributed to water stretching vibrations. A somewhat similar spectral pattern is observed for the infrared spectrum (Fig. 5b). A sharp infrared band is found at 3600 cm^{-1} and is assigned to the stretching vibration of OH units. A series of broadish infrared bands are observed at 2846, 3040, 3154, 3230, 3305, 3423 and 3532 cm^{-1}. These bands are assigned to water stretching vibrations. The basic structure of colemanite contains endless chains of interlocking BO$_2$(OH) triangles and BO$_3$(OH) tetrahedrons with the calcium, water molecules and extra hydroxides interspersed between the chains.

The Raman spectrum over the 1400–1800 cm^{-1} spectral range is displayed in Fig. 6a. The infrared spectrum over the 1200–

1800 cm^{-1} region is reported in Fig. 6b. The Raman spectrum shows a band at 1603 cm^{-1} assigned to the water bending mode. The spectrum perhaps suffers from a lack of signal. This, however, is not unexpected as water has a very low Raman scattering cross section. The infrared spectrum in this spectral region shows a band at 1610 cm^{-1} with a second component at much higher wavenumbers at 1690 cm^{-1}.

4. Conclusions

There are many borate minerals which have yet to have their vibrational spectra determined and their molecular structure assessed in terms of their vibrational patterns. In this work, we have

measured the Raman and infrared spectrum of colemanite $CaB_3O_4(OH)_3 \cdot H_2O$ over the complete spectral range. The basic structure of colemanite contains endless chains of interlocking $BO_2(OH)$ triangles and $BO_3(OH)$ tetrahedrons with the calcium, water and extra hydroxide units interspersed between these chains. This means that both trigonal and tetrahedral borate exists in the structure of the mineral. This structure determines the vibrational spectra of colemanite.

The mineral colemanite is characterized by a very intense sharp band at $3605 \, cm^{-1}$ attributed to the stretching vibration of OH units. Associated with this stretching vibration are the BOH out-of-plane bending modes found in the $740–800 \, cm^{-1}$ spectral region and the in-plane bending modes observed by Raman bands the $1300–1500 \, cm^{-1}$ spectral range. Both the Raman and infrared spectra of colemanite are characterized by multiple water stretching bands indicating that water plays an important role in the structure of colemanite.

It is important to characterize the wide range of boron containing minerals because of their uses in a very wide range of applications.

Acknowledgments

References

[1] M. Alkan, M. Dogan, Chem. Eng. Process. 43 (2004) 867.
[2] M.E. Back, J.A. Mandarino, Mineralog. Rec. (2008).
[3] P.C. Burns, F.C. Hawhorne, Can. Mineral. 31 (1993) 297.
[4] I. Waclawska, L. Stoch, J. Paulik, F. Paulik, Thermochim. Acta 126 (1988) 307.
[5] G. Gündüz, A. Usanmaz, J. Nucl. Mater. 140 (1986) 44.
[6] F. Demir, G. Budak, R. Sahin, A. Karabulut, M. Oltulu, A. Un, Ann. Nucl. Energy 38 (2011) 1274.
[7] S. Targan, A. Olgun, Y. Erdogan, V. Sevinc, Cem. Concr. Res. 33 (2003) 1175.
[8] N. Altar, A. Olgun, J. Hazard. Mater. 146 (2007) 171.
[9] M.G. Stamatakis, G. Economou, Econ. Geol. 86 (1991) 187.
[10] G.H. Hanks (Ed.), Third Annual Report of the State Mineralogist, 1833, pp. 81.
[11] C. Helvaci, R.N. Alonso, Turkish J. Earth Sci. 9 (2000) 1.
[12] J.D. Grice, R.A. Gault, J.V. Velthuizen, Can. Mineral. 43 (2005) 1469.
[13] I. Ardelean, S. Cora, J. Mater. Sci.: Mater. Electron. 19 (2008) 584.
[14] I. Ardelean, S. Cora, J. Optoelectron. Adv. Mater. 12 (2010) 239.
[15] I. Ardelean, L. Griguta, J. Optoelectron. Adv. Mater. 9 (2007) 2068.
[16] I. Ardelean, V. Timar, J. Optoelectron. Adv. Mater. 10 (2008) 246.
[17] F.H. El Batal, M.A. Azooz, A.A. El-Kheshen, Trans. Indian Ceram. Soc. 68 (2009) 81.
[18] F.H. ElBatal, Y.M. Hamdy, Trans. Indian Ceram. Soc. 67 (2008) 193.
[19] C. Rajyasree, P.M. Vinaya Teja, K.V.R. Murthy, D. Krishna Rao, Phys. B: Condens. Matter. (Amsterdam Netherlands) 406 (2011) 4366.
[20] B. Sumalatha, I. Omkaram, T.R. Rao, C.L. Raju, J. Non-Cryst. Solids 357 (2011) 3143.
[21] M. Mir, J. Janczak, Y.P. Mascarenhas, J. Appl. Crystallogr. 39 (2006) 42.
[22] I. Mitov, Z. Cherkezova-Zheleva, V. Mitrov, J. Balkan Tribol. Assoc. 4 (1998) 191.
[23] A.S. Povarennykh, E.I. Nefedov, Geol. Zh. (Russ. Ed.) 31 (1971) 13.
[24] V.S. Suknev, E.N. Diman, Zh. Prikl. Spektrosk. 10 (1969) 326.
[25] V.F. Ross, J.O. Edwards, Chem. Boron Compd. (1967) 15.
[26] R.L. Frost, J. Raman Spectrosc. 42 (2011) 540.
[27] M.V. Akhmanova, Zh. Strukt. Khim. 3 (1962) 28.
[28] D.A. Long, R.T. Bailey, Spectrochim. Acta 19 (1963) 1607.
[29] A. Vasko, I. Srb, Czech J. Phys. 17 (1967) 1110.
[30] C.E. Weir, Sect. A: Phys. Chem. 70 (1966) 153.
[31] V.C. Farmer, Mineralogical Society Monograph 4: the Infrared Spectra of Minerals. 1974.
[32] R.L. Frost, S. Bahfenne, J. Raman Spectrosc. 42 (2011) 219.
[33] R.L. Frost, S. Bahfenne, J. Cejka, J. Sejkora, J. Plasil, S.J. Palmer, E.C. Keeffe, I. Nemec, J. Raman Spectrosc. 42 (2011) 56.
[34] R.L. Frost, J. Cejka, J. Sejkora, J. Plasil, B.J. Reddy, E.C. Keeffe, Acta Part A 78 (2011) 494.
[35] R.L. Frost, S.J. Palmer, Acta Part A 78 (2011) 1250.
[36] R.L. Frost, S.J. Palmer, H.J. Spratt, W.N. Martens, J. Mol. Struct. 988 (2011) 52.
[37] R.L. Frost, J. Sejkora, J. Cejka, J. Plasil, S. Bahfenne, E.C. Keeffe, J. Raman Spectrosc. 42 (2011) 534.
[38] V. Devarajan, E. Gräfe, E. Funck, Spectrochim. Acta 30A (1974) 1235.
[39] L. Jun, X. Shuping, G. Shiyang, Spectrochim. Acta 51A (1995) 519.
[40] V. Bermanec, N. Tomašić, G. Žigovečki, L. Rajić, K. Furić, Mineral. Mag. 76 (2010) 1013.
[41] L. Frost Ray, Y. Xi, Spectrochim. Acta A Mol. Biomol. Spectrosc. 96C (2012) 611.
[42] L. Frost Ray, Y. Xi, Spectrochim. Acta A Mol. Biomol. Spectrosc. 96C (2012) 89.